Background at Future Linear Colliders

D. Schulte

CERN, CH-1211 Geneva, Switzerland
E-mail: Daniel.Schulte@cern.ch

Abstract

Detector background in future linear e^+e^--colliders, as will arise for example from the beam-beam interaction, will strongly affect experimental conditions. A short overview of the main background sources is given. Numerical results are presented, mainly for TESLA at a centre-of-mass energy $E_{cm} = 0.5\,\mathrm{TeV}$ and for CLIC at $E_{cm} = 3\,\mathrm{TeV}$.

---

1 Introduction

A number of international working groups are studying the feasibility of future high energy linear e^+e^--colliders [1], as well as the conditions for physics experiments on these machines. The main studies are TESLA [2], JLC [3], NLC [4], and CLIC [5]. The main parameters of these projects are shown in Table 1. In all these machines a train of bunches is accelerated by each RF-pulse in order to achieve high efficiency. The detectors will therefore see short bursts of high luminosity followed by pauses of some milliseconds.

In the following, an overview over the most important sources of background in the detector at these machines is given. The emphasis will be on TESLA and CLIC, the studies presented in this meeting.

1.1 Different Studies

TESLA is a machine that uses superconducting accelerating structures in the main linac, making it possible to have an efficient transformation of RF-power into beam power. To preserve the emittance of a beam during acceleration is relatively simple due to low wakefields in the structures, this in turn allows high luminosity. Due to the very high Q-value of the superconducting structures, the total length of the pulse train is 0.8 ms, leading to a distance between bunches of about $\Delta_b \approx 300\,\mathrm{ns}$. This makes different bunch crossings distinguishable in most detector components. It also allows head-on collision of the beams, since the outgoing bunch can be separated from the next incoming outside of the detector.

In a joint study by ECFA and DESY, the physics potential of TESLA has been investigated [2][7]. A second study is carried out currently [6]. A complete detector simulation exists, named BRAHMS [8] and background simulations are well advanced [9].

The normal conduction machines do differ from one another in their acceleration frequencies, but efficiencies and background conditions remain comparable at the same

Table 1: The parameters of the main projects. Some of them actually have a variety of parameter sets, JLC even two acceleration frequencies.

name		TESLA		NLC/JLC		CLIC	
E_{cm}	[TeV]	0.5	0.8	0.5	1.0	0.5	3.0
$\mathcal{L}$	$[10^{34}\text{cm}^{-2}\text{s}^{-1}]$	3.1	5.7	0.65	1.3	1.4	10.0
f_{RF}	[GHz]	1.3	1.3	11.4	11.4	30	30
G_{load}	[MV/m]	21.7	34	55	55	150	150
η	[%]	23	18	8.9	8.6	9.9	9.9
f_r	[Hz]	5	3	120	120	200	100
N_b		2820	4500	95	95	154	154
Δ_b	[ns]	337	189	2.8	2.8	0.67	0.67
N	$[10^{10}]$	2.0	1.4	0.95	0.95	0.4	0.4
σ_z	$[\mu\text{m}]$	400	300	120	120	30	30
ϵ_x	$[\mu\text{m}]$	10	8	4.5	4.5	2.0	0.68
ϵ_y	$[\mu\text{m}]$	0.03	0.01	0.1	0.1	0.02	0.02
σ_x^*	[nm]	553	391	332	235	202	43
σ_y^*	[nm]	5	2	5	4	2.5	1
δ	[%]	2.8	4.7	3.8	9.1	4.4	31
n_γ		1.6	1.5	1.2	1.5	0.7	2.3
$N_\perp$		44	63	9.8	18.4	4.4	60
N_H		0.23	0.6	0.07	0.33	0.047	4.05
N_{MJ}	$[10^{-2}]$	0.61	3.1	0.20	2.3	0.24	340

E_{cm}: centre-of-mass energy, $\mathcal{L}$: actual luminosity, f_r: repetition frequency, N_b: number of bunches per train, Δ_b: distance between bunches, N: number of particles per bunch, σ: bunch dimensions at IP, $\gamma\epsilon$: normalised emittances, Υ: average beamstrahlung parameter, δ: average energy loss, n_γ: number of photons per beam particle, $N_\perp$: number of particles from incoherent pair production, produced with $p_\perp >$ $20\,\text{MeV}, \theta > 0.15$, N_{Hadr}: number of hadronic events, N_{MJ}: number of minijet pairs $p_\perp > 3.2\,\text{GeV/c}$.

energies. Efficiencies are lower than that of TESLA by roughly a factor two and the pulse lengths are very short, leading to a bunch-to-bunch distance of $0.67 - 2.8\,\text{ns}$. It is thus more difficult to distinguish different bunch crossings. In order to avoid the outgoing bunches kicking the incoming ones, it is also necessary to have a crossing angle between the two beam lines. CLIC differs from the other machines because of the high centre-of-mass energy aimed for, which leads to completely new conditions for the beam-beam interaction.

For JLC [10] and NLC [11] studies of the physics and the background conditions are also performed. Their status is fairly advanced including detector simulations. For CLIC background studies have started only recently [12].

1.2 Background

The detector background can be divided into the part that is produced by the accelerator complex before the interaction point, the part due to beam-beam interaction and the part due to the spent beam after the interaction.

Beam tails from the main linac fall into the first category. These particles can be lost in the beam line or in the worst case in the detector. To avoid this, the beams have to be collimated before the final focus system in the collimation section. Secondary muons can also lead to significant background as experienced at the SLC. Synchrotron radiation emitted by the beam in the beam delivery system is another background source. Collimators can be used to protect the interaction region if the photons are emitted upstream of the final doublet. Photons emitted in the final doublet cannot be collimated but most of these photons will pass through the detector without interacting. Only photons emitted by particles in the beam tails could hit material in the detector. Collimation of the main beam can therefore solve this problem and sets the tightest transverse collimation requirements. Due to scattering of beam particles off rest gas and thermal photons, additional beam tails can be produced inside the beam delivery region.

The intense electromagnetic fields created in the interaction point during the bunch crossing lead to beamstrahlung. While this radiation does not form a background source for the detector directly, secondaries do. The main effect is from coherent and incoherent pair creation and production of hadrons. Also secondary neutrons are of concern.

The spent beam can lead to production of secondary background. Neutrons are produced by beam losses in the collimators along the transport line and in the beam dump. Careful shielding of the detector is therefore necessary.

2 Machine Background

The background level due to the machine needs careful evaluation and development of means to reduce it. It can to a large extend be influenced by the design of the beam delivery system.

2.1 Beam Tails

Particles in the tails of the beams can hit the detector and it is therefore necessary to remove them from the beam by collimation. The collimation section also serves as a part of the machine protection system. In all projects, one of the initial requirements was that the collimators should be able to stop a mis-steered beam without being destroyed. In the studies it was found very difficult, if not impossible, to fulfil this goal. The collimators are able to protect the detector and the rest of the machine, but they can be destroyed. Therefore, the strategy at NLC is to consider consumable or renewable collimators. The former, for example, in the form of a cylindrical collimator. After accidental destruction of its surface by the beam, it is rotated moving a new part of the surface towards the beam. This would allow for about one thousand accidents before the collimators have to be replaced. However, the solution is technically difficult. In the renewable solution, the surface of the collimator is covered by a thin metal film. The collimator is again a rotating cylinder were the metal film is continually replaced by a new one outside of the beam pipe in a liquid metal bath. This solution seems even more difficult than the first.

For TESLA a design of the collimation system exists; but it is necessary to improve this to meet the new requirements for the high-luminosity parameters. This requires a significant amount of work. For CLIC nothing has been done so far.

2.2 Synchrotron Radiation

The beam particles emit synchrotron radiation in the magnets of the beam delivery line. The number of these photons can be of the same order as the number of particles in the

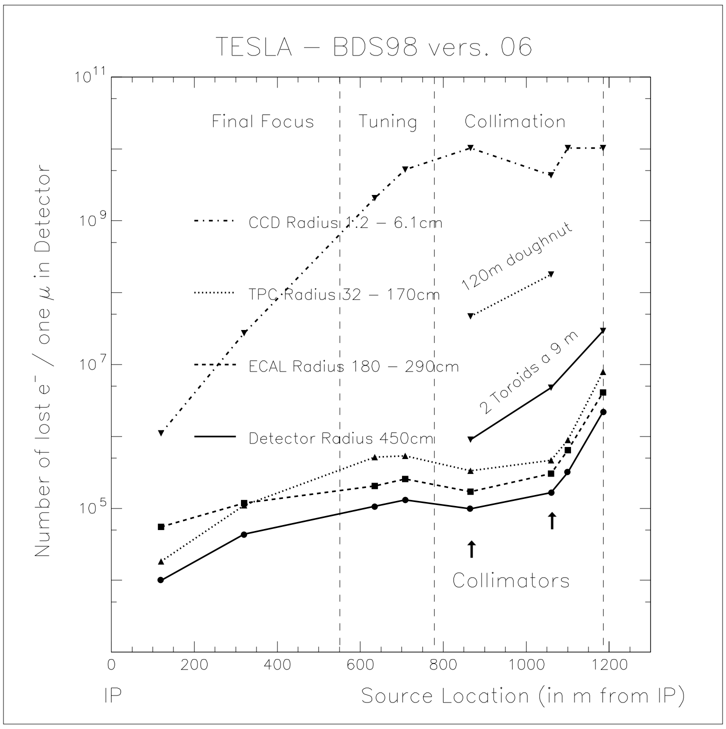

Figure 1: The number of electrons one can loose in order to produce one muon in the detector as a function of the position. The plot was taken from a presentation of N. Tesch[35].

beam. The photons as well as their secondaries must be collimated before the detector, allowing only third generation background to enter the detector. In the case of TESLA one has to be cautious because of the immense power of the beamstrahlung coming from the detector. This is a hazard for the collimators. In the other designs this is of no concern, since incoming and outgoing beam lines are different. The neutrons, produced by losses of the spent beam and the beamstrahlung, form another source of background in the detector. For CLIC neither a fixed final focus system nor an extraction beam line design exists, so no work has been done designing the photon collimation system.

The photons emitted by the beam in the final doublet are a special problem, since they cannot be collimated. One has therefore to make sure that they can leave the detector through the doublet downstream of the interaction point. This can be achieved by collimating the beam tails, thus preventing the particles following trajectories on which they can emit photons that hit the opposing doublet. This defines the aperture requirements for the beam collimation section.

2.3 Muon Production

Muons can be produced via the Bethe-Heitler process if electrons hit material. While one tries to minimise the beam losses along the beam delivery system, one certainly cannot avoid them in the collimation system. Different programs exist to simulate the production and transport of the muons along a beam line [13][14]. Since the sizes of the beam tails are unknown, the number of electrons that can be lost to produce one muon on average in the detector is plotted versus the position along the beam line. As can be seen in Fig. 1, this number depends strongly on the position. The number of muons can be significantly reduced by adding material into the tunnel, as for example magnetised spoilers.

For TESLA and NLC many simulations of the muon background have been done. Still, since the sizes of the tails to be collimated are not known, one cannot predict the level of muon background in the detector. For TESLA, known processes predict a low number of particles in the tails, so the rate would be very small, about one muon per bunch crossing. Expensive spoilers would be only installed if necessary. Fine granularity allows the detector to operate in high muon flux, but increases the cost significantly.

For CLIC no calculations have been done until now. Depending on the detector design, the flux of muons per bunch train rather than per bunch will have to be taken into account.

2.4 Beam-Gas and Beam-Black Body Radiation Scattering

Beam particles can scatter off residual gas in the beam pipe which can lead to a significant energy loss. Particles scattered in the final focus system will not be removed from the beam and can therefore cause background. The rate due to this process is proportional to the vacuum pressure. Beam particles can also scatter on thermal photons. This rate can only be influenced by varying the temperature of the beam pipe. At a vacuum pressure of about 10^{-9} Torr, the rates from beam-gas scattering and beam-black body radiation scattering at room temperature should be comparable[15].

Tracking of the secondaries is necessary to evaluate the effects of these two processes. This remains to be done.

3 Beam-Beam Effects

In future linear colliders, the bunches collide only once. They must therefore have small cross sections in order to achieve high luminosity. This leads to strong beam-beam effects and subsequently to high background. Possible means to suppress these effects are discussed, but none of them is in a state that it could realistically be proposed.

3.1 Pinch Effect

During collision in an electron-positron collider, the particles of each beam are accelerated towards the transverse centre of the oncoming bunch by its electric and magnetic forces. In the proposed colliders this effect is so strong that the transverse dimensions of the bunches are significantly reduced during the collision, the so-called pinch effect. This enhances the luminosity typically by a factor 1.5–2. Simulation programs have been developed to investigate this effect[16][17]. They also include most of the background sources described later. The pinch effect calculated by these programs has been successfully compared to SLC data [18].

Since the particles travel on curved trajectories, they emit beamstrahlung which is comparable to synchrotron radiation. The number of emitted photons is typically of the order of one per beam particle and they have energies of a few GeV. During collision, particles lose on average between 2.5 % of their energy in TESLA at $E_{cm} = 0.5$ TeV and 40 % in CLIC at $E_{cm} = 5$ TeV.

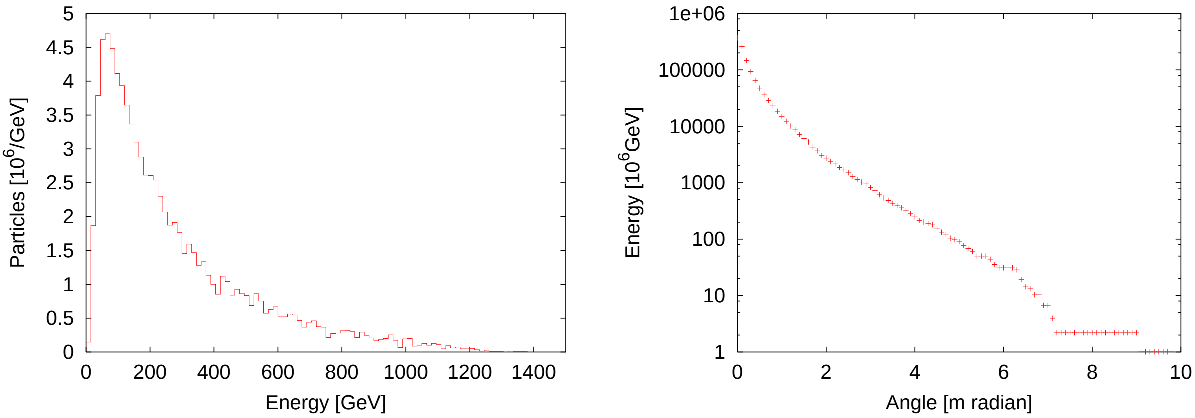

Figure 2: The energy spectrum and transverse distribution of the coherent pair particles in CLIC at $E_{cm} = 3\,\text{TeV}$.

3.2 Coherent Pair Creation

A high-energy photon can turn into an electron-positron pair in a strong electromagnetic field. For machines with a centre-of-mass energy of 1 TeV or less, this effect either forms only a small background or is not important at all. At high energies, the number of produced particles is significant compared to the original bunch charge and has to be included in the simulations.

For CLIC, GUINEA-PIG predicts 700, $3 \cdot 10^6$, $7 \cdot 10^8$ and $2 \cdot 10^9$ pairs per bunch crossing for $E_{cm} = 0.5$, 1, 3 and 5 TeV, respectively. The spectrum of the particles at $E_{cm} = 3\,\text{TeV}$ peaks at $E \approx 50 - 100\,\text{GeV}$, as shown in Fig. 2. Generated pairs initially have small angles. An electron flying in the electron beam direction is focused by the oncoming positron beam and thus starts to oscillate. A positron flying in the same direction is defocused and can consequently reach relatively large angles. While these particles can only hit the quadrupoles, secondaries can be a hazard to the detector. The final quadrupoles provide an (almost field free) exit hole. In Fig. 2, the total energy of coherent particles per bunch crossing is shown as a function of the minimum particle angle. For comparison, in TESLA at $E_{cm} = 0.5\,\text{TeV}$ the total energy lost in the detector per bunch crossing is of the order $10^6\,\text{GeV}$, mainly from incoherent pair production and bremsstrahlung. To reach a comparable level in CLIC, an exit hole with an opening angle of the order of 10 mradian is necessary. In this case the effects of secondaries should also be comparable to those in TESLA.

3.3 Luminosity Spectrum

To illustrate the effect of the luminosity spectrum, the resolution of a top threshold scan is shown in Fig. 5. An event reconstruction efficiency of 50 % is assumed and only the total cross section is used, as calculated with the code RTOP [19][1]. Initial state radiation increases the uncertainty by fifty percent, and beamstrahlung and beam energy spread give about the same effect. The possible trade off between total luminosity and spectrum is shown in the same figure on the right hand side. Different horizontal beam

[1] It should be noted that the predicted resolution with the more complete program TOPPIK [20], as used for the TESLA calculation, is better than the one predicted by RTOP. Here, only the relative results are important.

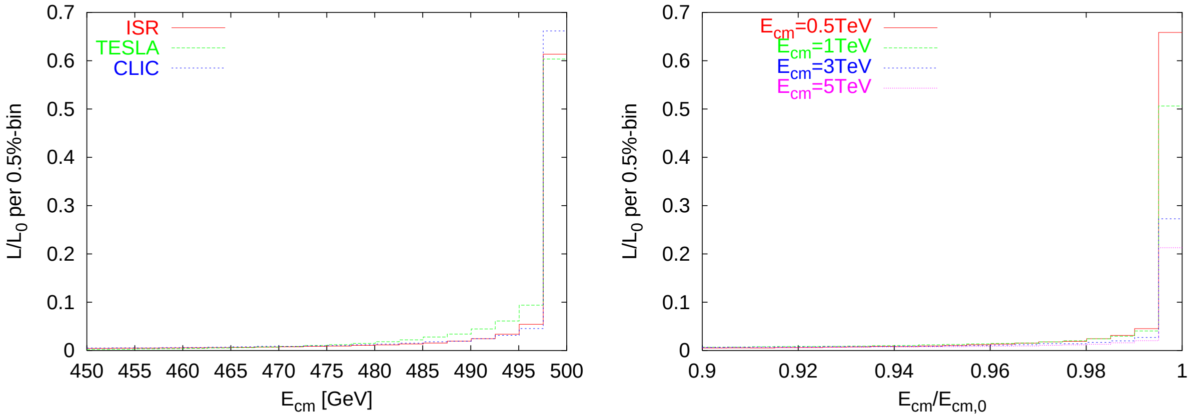

Figure 3: Luminosity spectrum for TESLA and CLIC at $E_{cm} = 0.5\,\mathrm{TeV}$ (left) and for CLIC at all energies (right).

Because of the energy loss due to beamstrahlung, the centre-of-mass energy of the electron-positron collisions can differ from the nominal one. A similar effect arises from initial state radiation. In all low energy designs the beamstrahlung is kept to a level where it is comparable to initial state radiation, see Fig. 3. At high energies, the energy loss has to be larger in order to achieve high luminosity. It is possible to trade off luminosity versus sharpness of the energy spectrum. In Fig. 4, the absolute and relative luminosities with $E_{cm} > 0.99E_{cm,0}$ and $E_{cm} > 0.95E_{cm,0}$ are shown for different transverse beam sizes σ_x in the case of CLIC at $E_{cm} = 3\,\mathrm{TeV}$. Inherent beam energy spread and initial state radiation are ignored in this comparison. In order to determine the best parameters, evaluation of possible experimental analysis is necessary.

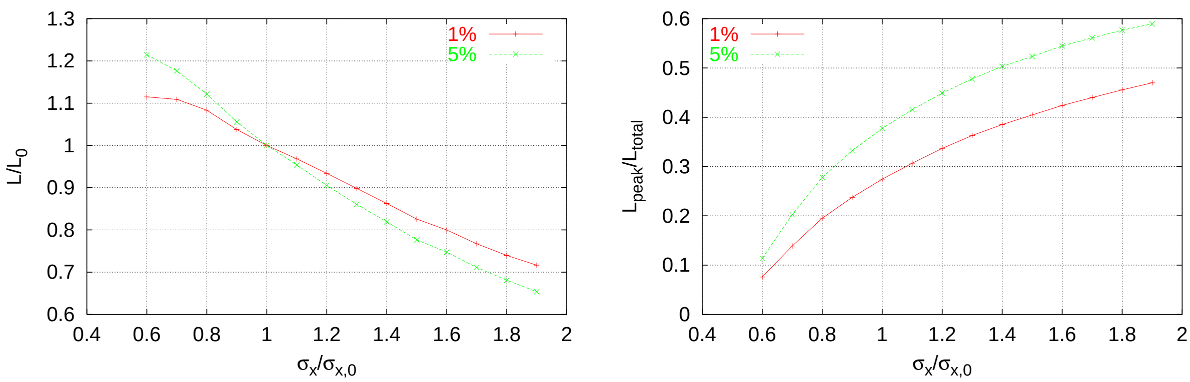

Figure 4: The total and fractional luminosity close to the nominal centre-of-mass energy as a function of σ_x. The total luminosity is normalised to the one expected for the nominal parameters.

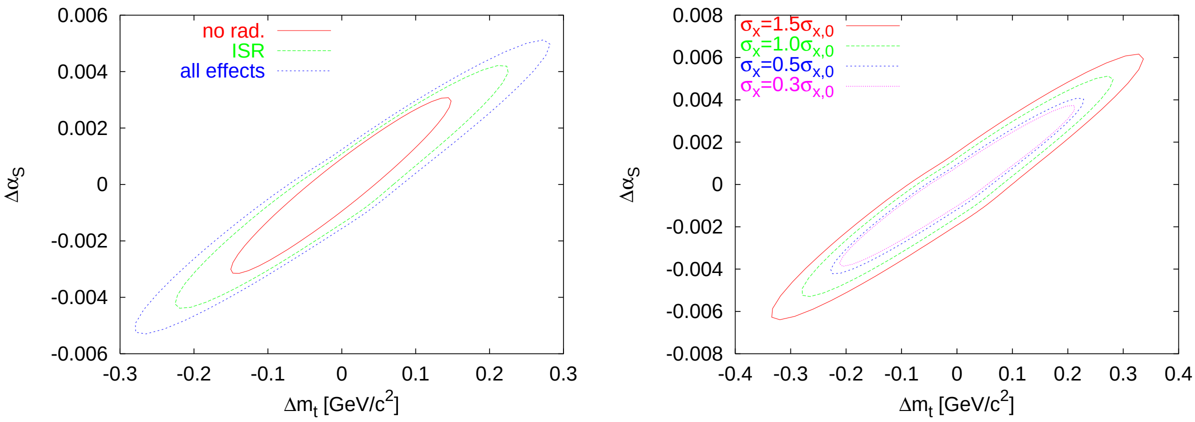

Figure 5: Resolution of the top threshold scan using nine scanning points (plus one for background estimation) with one day of data taking for each. The $\Delta\chi^2 = 1$-contour is shown for a simultaneous fit of the strong coupling α_S and the top mass m_t. The beam parameters are from an older parameter set of CLIC.

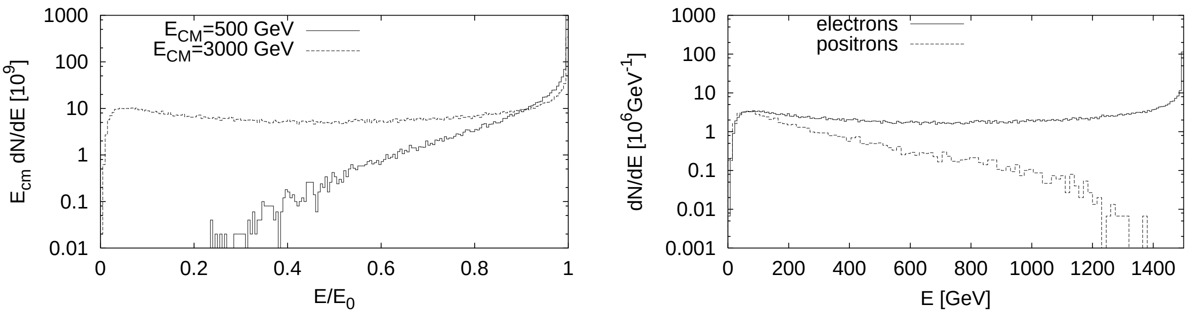

Figure 6: The energy spectrum of the spent beam at different centre-of-mass energies (left). The spectrum of electrons and positrons in the spent electron beam at $E_{cm} = 3$ TeV.

sizes are assumed for otherwise unchanged parameter sets. A large σ_x corresponds to low luminosity with a good spectrum. The case with the highest beamstrahlung is best, since the gain in luminosity outweighs the smearing of the spectrum. With TESLA, it should be possible to achieve a resolution of $\Delta_t \approx 100\,\mathrm{MeV/c^2}$ with about $50\,\mathrm{fb}^{-1}$[21].

The luminosity spectrum is available in standard generators, as for example PYTHIA, via the program CIRCE [22], which uses fits to GUINEA-PIG results.

3.4 Spent Beam

Due to the pinch effect, the transverse emittances of the beam will be significantly increased after the collision. In addition, particles can lose a significant fraction of their energy. The beam line that extracts the spent beam from the interaction point must be able to transport all these different energies. For TESLA, a spent beam extraction line has been designed that can transport the beam to the beam dump.

Figure 6 shows the energy spectrum of the beam particles in CLIC after the interaction for $E_{cm} = 0.5$ TeV and $E_{cm} = 3$ TeV. The first case is comparable to the NLC at $E_{cm} = 1$ TeV for which a solution exists [23]. At high energy, the number of particles at very low energies becomes significant. A large fraction of these particles is produced by coherent pair production, as can be seen on the right hand side of Fig. 6. This

name		TESLA		NLC/JLC		CLIC	
E_{cm}	[TeV]	0.5	0.8	0.5	1.0	0.5	3.0
N_{pairs}	10^3	160	242	39.5	92	21	455
E_{pairs}	10^3 GeV	310	1070	124	965	113	38500

Table 2: Number and total energy of the pair particles per bunch crossing for the different machines.

further complicates the design of the extraction line, since both signs of charge have to be transported. Again, this problem has not yet been studied.

4 Background due to Beam-Beam Interaction

While the background from coherent pair creation and the spent beam can be reduced by adequate design of the line for the spent beam, this is not possible for the processes described below.

The number and total energy of the pair particles produced per bunch crossing are listed in Table 2.

4.1 Incoherent Pairs

The production of e^+e^- pairs through two photon processes can lead to significant background at all energies. The main contributions arise from ee $\rightarrow$ ee(e^+e^-), e$\gamma \rightarrow$ e(e^+e^-) and $\gamma\gamma \rightarrow$ (e^+e^-). The photons are from beamstrahlung. The processes involving one or two beam particles can be approximately calculated using the equivalent photon approach. This also allows taking into account the effects of the beam size and the strong beam field onto the cross section.

As for the coherent pairs, it is necessary to track the produced particles through the fields of the two beams. Each dot in Fig. 7 represents one particle after the bunches crossed. For the bulk of the particles, a clear correlation between the maximum transverse momentum and angle reached is visible. The few particles above this edge were produced with large angles and transverse momenta. Those below the edge obtained most of their transverse momentum from the deflection by the beams.

4.2 Impact on the Detector

Incoherent pairs can have rather large angles with respect to the beam axis, producing significant background in the detector, especially in the vertex detector. On the right hand side of Fig. 7, the density of particles that hit the inner layer of a vertex detector is shown as a function of the radius of this layer (CLIC at $E_{cm} = 3\,\mathrm{TeV}$). The angular coverage is kept constant at $|\cos\theta| \leq 0.98$ and different magnetic fields are used. Due to the field the particles travel on helixes. The particles with a large angle tend to have a small transverse momentum, this limits the distance they can reach from the beam axis. The steep rise, observed in each of these curves, corresponds to the edge in the scatter plot in Fig. 7. In order to avoid the bulk of the particles, the radius of the vertex detector has to be sufficiently large. The longitudinal distribution of actual hits produced by the particles is shown in Fig. 8, based on GEANT simulations of a magnetic field of 4 T and different radii. The density is relatively uniform except for low radii where the ends of the

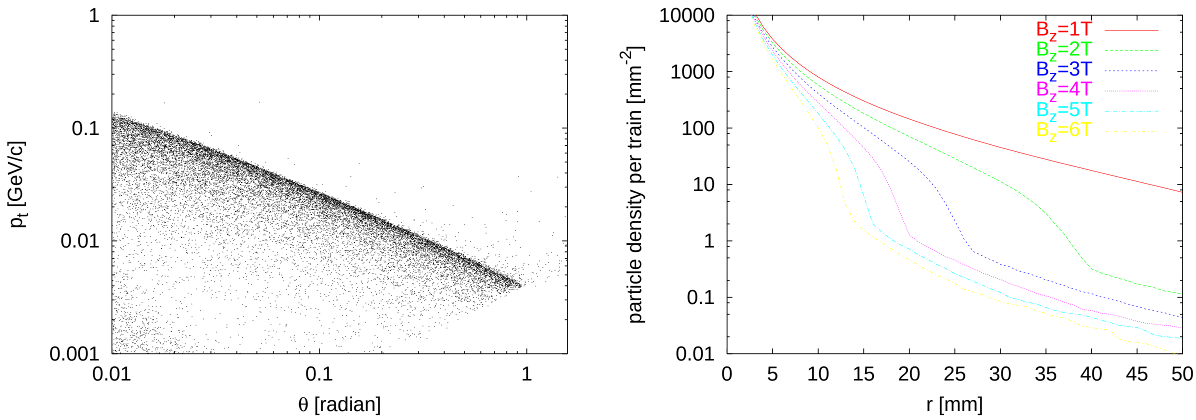

Figure 7: Particles from incoherent pair creation after the collision (CLIC at $E_{cm} = 3\,\mathrm{TeV}$). Each dot presents one particle. On the right hand side the number of particles is shown that hit the inner layer of the vertex detector as a function of the radius. Different magnetic fields are assumed for the detector solenoid. The detector half-length is always $z = 5r$, given a coverage of $|\cos\theta| \leq 0.98$.

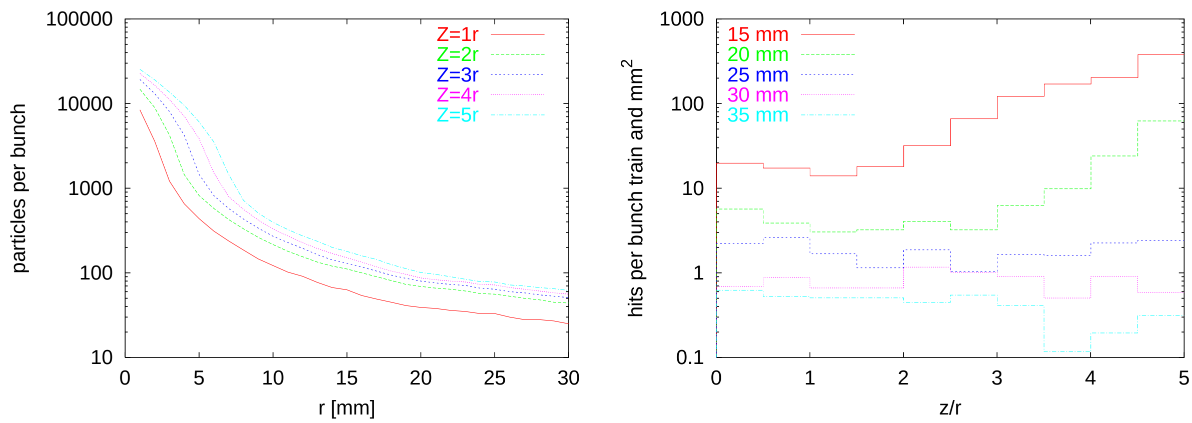

Figure 8: The longitudinal distribution of the hit density is shown for a detector magnetic field $B_z = 4\,\mathrm{T}$ in the case of CLIC at $E_{cm} = 3\,\mathrm{TeV}$. On the right hand side, the particle density in the vertex detector of TESLA at $E_{cm} = 500\,\mathrm{GeV}$ is shown as a function of the detector radius. Different coverage angles are assumed.

detector are hit by the deflected particles. By increasing the opening angle of the detector one can therefore allow smaller radii without increasing the number of hits drastically, as shown on the left hand side of Fig. 8.

In a normal conducting machine, the vertex detector will be likely to consist of charged coupled devices (CCDs). During the luminosity pulse which lasts a few hundred nanoseconds, LHC-type pixel detectors can be read out only few times, so they gain relatively little advantage. CCDs, on the other hand, have a very high granularity which allows good track reconstruction even in the presence of a large number of background hits. The read-out time of the order of milliseconds matches well with the time between pulses. One can accept about one hit per mm^2 in a CCD detector [25]. In CLIC at $E_{cm} = 3\,\mathrm{TeV}$ one can therefore allow an inner radius of the vertex detector of about 30 mm, see Table 3. In JLC a radius of 24 mm leads to acceptable background while the numbers found for NLC at 12 mm are somewhat high, with a large fraction of the hits being due to secondaries

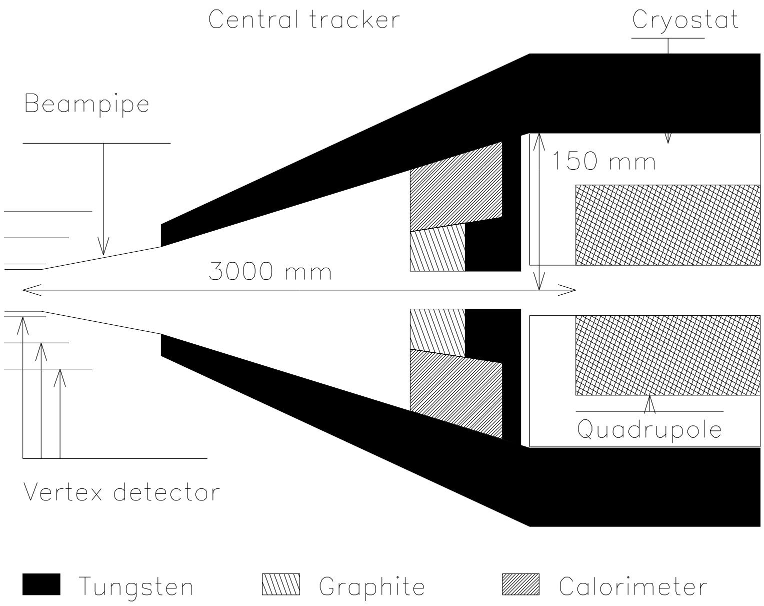

Figure 9: The masking system as foreseen for TESLA, the one for CLIC is expected to have similar properties.

from the final quadrupoles. In TESLA the situation is more complicated since the total amount of background during one pulse is very high. Here, one has to take advantage of the long pulse duration which allows more frequent reading of the detectors.

Most of the particles from pair creation hit a small area in the front and back of the detector, but their secondaries can cause significant background. To prevent this, the final quadrupoles are surrounded by tungsten masks, as in Fig. 9. The thickness of these masks needs to be about 5–10 cm [29]. The outer angle of this mask can be as low as 83 mradian in TESLA.

Low energy electrons and positrons are also scattered back. The field of the main solenoid guides these particles directly into the vertex detector region, as it guided the low energy particles out in the first place. The increase of hits in the inner layer of the vertex detector due to this effect can be a factor ten. However, almost complete suppression of the backscattering can be achieved by introducing an inner mask, with an inner radius smaller than that of the vertex detector [29]. In the case of TESLA, this mask consists of a tungsten layer towards the quadrupoles and layer of a low-Z material towards the detector. Charged particles penetrate this layer with a small probability of interaction. So, low energy secondaries have to pass a significant length of material loosing energy by ionisation before exiting the mask. For CLIC and JLC[26] similar systems are foreseen, even so for CLIC they are not yet simulated. NLC will likely also use an equivalent mask[28]. This should solve the problem of the high hit density mentioned before. This inner mask should be instrumented in order to be able to measure the total electromagnetic energy deposited in it for luminosity instrumentation as will be explained below.

	NLC	JLC	TESLA	CLIC
E_{cm} [TeV]	1.0	0.5	0.5	3.0
B_z [T]	6	2	3/4	4
r [mm]	12	24	12	30
n_h [$\mathrm{mm}^{-2}\mathrm{BX}^{-1}$]	0.1	0.01	0.2/0.1	0.005*
n_h [$\mathrm{mm}^{-2}\mathrm{Train}^{-1}$]	10	1	560/280	0.8*

* direct hits only

Table 3: Hit density in the innermost layer of the vertex detector for different machines. NLC has severe background from backscattered particles. JLC has only low field. TESLA cannot accept to read out once per train but much more frequent. CLIC needs larger radius because of high energy and high N/σ_z. Values are taken from [27], except for CLIC.

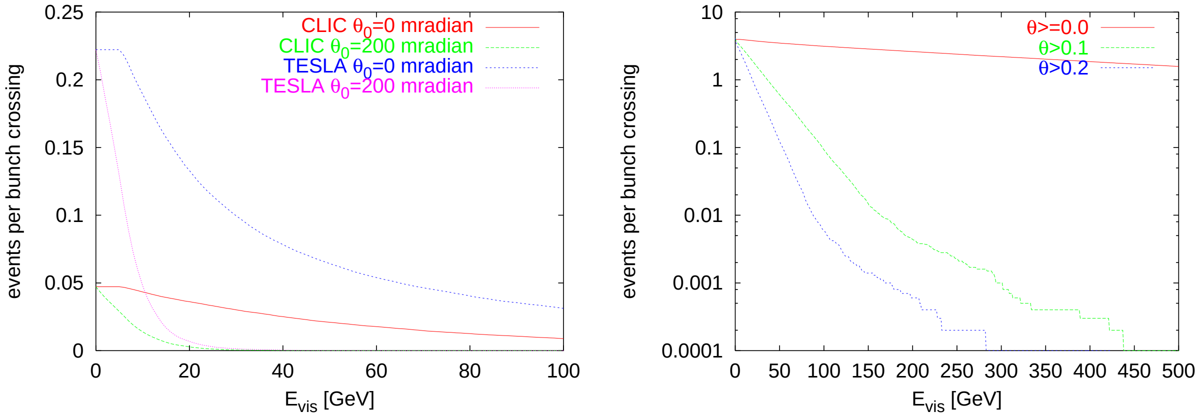

Figure 10: The average number of hadronic events per bunch crossing as a function of the visible energy, on the left hand side for a centre-of-mass energy of $E_{cm} = 500\,\mathrm{GeV}$, on the right hand side for $E_{cm} = 3\,\mathrm{TeV}$.

4.3 Measuring the Luminosity

A fast relative measurement of the luminosity is necessary to be able to tune beam parameters during operation. The transverse offsets between the two beams in the interaction point can be easily determined using beam position monitors and corrected using small kicker magnets. An increase of the spot size is more difficult to detect. A common source for spot size increase is a longitudinal shift of the vertical beam waist.

Several signals can in principle be used to optimise the luminosity [30]. For example measuring the rate of particles that emitted bremsstrahlung of a certain hardness. Also the total energy deposited by the incoherent pairs in the inner mask can be used. Maximising it, by changing the position of the vertical waist for example, leads to optimal luminosity. The beamstrahlung can be used in some cases but not as straightforwardly as the other options. For all projects complete investigation of these options in the presents of different error sources have to be investigated in more detail.

4.4 Hadronic Background

In high-energy two-photon collisions also hadrons are produced. The photon can interact as a point-like particle, but in most cases one or both of the photons interact as hadrons (once- and twice-resolved processes). For the total cross section different estimates exist, the one used here is a pessimistic version of a parametrisation due to Schuler and Sjöstrand [31]. With GUINEA-PIG the number of events can be calculated and they can be fully simulated with the help of PYTHIA [32]. Other studies concentrate on simulating the hardest part of the events, the minijet events [33]. This allows detailed studies of their effects on the reconstruction of interesting events. The number of events per bunch crossing with a centre-of-mass energy in excess of 5 GeV is $N_{had} = 0.23(0.6)$ for TESLA at $E_{cm} = 500\,\mathrm{GeV}(800\,\mathrm{GeV})$, $N_{had} = 0.07(0.33)$ for NLC/JLC at $E_{cm} = 500(1000)\,\mathrm{GeV}$ and $N_{had} = 0.047(4.05)$ for CLIC at $E_{cm} = 500(3000)\,\mathrm{GeV}$.

The resulting distributions of visible energy for TESLA and CLIC are shown in Fig. 10. The number of events per bunch crossing is significantly lower than one at $E_{cm} \leq 1\,\mathrm{TeV}$ but increases drastically towards higher energies (≈ 4 in CLIC at $E_{cm} = 3\,\mathrm{TeV}$). In the normal conducting designs very fast detectors are necessary to distinguish the different bunch crossings. While most of these events produce visible energy, only a small fraction, the minijet events, are hard. As soon as a small angle cut is used, the event rate is drastically reduced.

Hadronic background especially affects the reconstruction of masses. In case part of the final state particles are invisible (as for example in $\mathrm{e^+e^-} \rightarrow \mathrm{h}\nu\bar{\nu}$) this can lead to significant changes of the measured signal [34]. However, more complete studies have to be done which include means of reducing the background. For example, one can try to estimate the likelihood of the event being overlaid by a background event and react accordingly. In the case of TESLA the number of background events is relatively high for the centre-of-mass energy, but the long bunch allows the use of the longitudinal position differences between the jets to differentiate background jets from interesting ones.

In the top threshold scan, the background can increase the rate of non-top events which are incorrectly accepted as top events [29]. One background event per bunch crossing will increase the rate of wrongly accepted events by about 50 %. The resulting effect on the resolution is very small.

4.5 Neutrons

Neutrons are produced in the electromagnetic showers induced by the electrons and positrons lost in the final quadrupoles. For most detector components, radiation levels are very low, but the neutrons can be a hazard for a CCD based vertex detector and a background source for the end-cap calorimeter. A study of the TESLA detector indicated that the neutron levels were acceptable but close to the limit for CCDs [29]. Also showers induced by the beamstrahlung photons in the collimators can cause problems, but the study indicated that the inner mask can shield the vertex detector sufficiently.

A more complete study [35] gives even lower values for a new and more favourable geometry. Similar studies have been carried out for JLC [36] and NLC [37]. The values found for NLC are two orders of magnitude higher than the ones for JLC. Clearly, more work has to be done, even though all studies indicate the neutron levels are low or at least acceptable.

5 Conclusion

The studies of the background at $\mathrm{e^+e^-}$ linear colliders are well advanced at energies up to $E_{cm} = 1\,\mathrm{TeV}$. The main missing components are the beam collimation systems.

Detector simulation programs and generators for the main background sources exist that allow sophisticated investigations. The effect of beamstrahlung can be simulated with standard event generators. Designs of the masks inside the detector exist for NLC, JLC and TESLA. The latter two achieve sufficiently low background, while NLC should be able to solve the remaining problem by changing the mask design. Further optimisations will be made for all these designs. For CLIC no masking system exists so far, but it should be straightforward to use the experience of the other studies. To gain more insight, reconstruction of interesting events including background has to be done. For JLC, NLC and TESLA, this should lead to realistic estimates of the precision of the measurements, as for example in the case of $e^+e^- \rightarrow h\nu\bar{\nu}$ with hadronic background. In the case of CLIC more basic investigations have to be initiated. The study of $E_{cm} = 3\,\mathrm{TeV}$ has only just begun, and at high energies coherent pair creation plays an important role and background levels increase significantly.

References

[1] `http://www.slac.stanford.edu/xorg/ilc-trc/ilc-trchome.html`

[2] R. Brinkmann et al. *DESY-1997-048* and *ECFA 1997-182*.

[3] The report of the JLC Design Study Group can be found on `ftp://lcdev.kek.jp/pub/DesignStudy/`.

[4] The NLC Design Group. *SLAC-Report 474*.

[5] J.-P. Delahaye et al. *PAC 1999* and *CERN/PS/99-05(LP)*.

[6] `http://www.desy.de/conferences/ecfa-desy-lc98.html`

[7] *DESY-123 A-E*

[8] BRAHMS is developed by G. Blair. It can be found at `http://www.hep.ph.rhbnc.ac.uk/b̃lair/detsim/brahms.html`

[9] O. Napoly, I. Reyzl, N. Tesch. *Proceedings of the International Workshop on Linear Colliders (LCWS99), Sitges, Spain; April 28 - May 5, 1999; to be published in World Scientific*

[10] `http://acfahep.kek.jp/`

[11] `http://lcwws.physics.yale.edu/lc/america.html`

[12] D. Schulte. *Proceedings of the International Workshop on Linear Colliders (LCWS99), Sitges, Spain; April 28 - May 5, 1999; to be published in World Scientific*

[13] S.H. Rokni, L.P. Keller and W.R. Nelson. *SLAC-PUB-7054*.

[14] M. Sachwitz and H.J. Schreiber. *TESLA-94-27*.

[15] H. Burkhardt. *CLIC-Note 416*.

[16] CAIN. Program is developed by K. Yokoya and others, see
`http://www-acc-theory.kek.jp/members/cain/`.

[17] GUINEA-PIG. D. Schulte. *CERN/PS/99-014-LP*. Available under
`http://www-sldnt.slac.stanford.edu/nlc/beamdeliveryhome.htm`

[18] T. Barklow and 14 co-authors. *PAC 1999* and *SLAC-PUB-8043*.

[19] RTOP was written by M. Peskin.

[20] TOPPIK was writen R. Harlander and M. Jezabek with earlier contributions from Th. Teubner.

[21] A. Juste, M. Martinez and D. Schulte. *DESY-97-123-e (1997)*.

[22] CIRCE was written by T. Ohl, see
`http://heplix.ikp.physik.tu-darmstadt.de/nlc/beam.html`

[23] Y. Nosochkov, T. Raubenheimer, K. Tompson and M. Woods. *Particle Acclerator Conference, New York 1999*

[24] D. Schulte. *CERN-PS-99-017-LP (1999)*.

[25] C. Damerell. Private communication.

[26] Y. Sugimoto. Talk presented at the LCWS99 in Sitges (1999), to be published in *World Scientific*.

[27] O. Napoly. Summary talk of the interaction region working group at the LCWS99 in Sitges (1999).

[28] T. Markiewicz and T. Maruyama. Private Communication.

[29] D. Schulte. *TESLA 97-08*.

[30] O. Napoly and D. Schulte. *Linac 98* and *DAPNIA-SEA-97-14*.

[31] G. A. Schuler and T. Sjöstrand. *CERN-TH/96-119*.

[32] T. Sjöstrand. *Computer Physics Commun. 82 (1994) 74*.

[33] J. Butterworth and W. Da Silva. Talks presented at the LCWS99 in Sitges (1999).

[34] S.Yamashita. Talk presented at the LCWS99 in Sitges (1999), to be published in *World Scientific*.

[35] N. Tesch. Talk at the LCWS99 in Sitges (1999), to be published in *World Scientific*.

[36] Y. Sugimoto. Talk at the LCWS99 in Sitges (1999), to be published in *World Scientific*.

[37] T. Maruyama. Talk at the LCWS99 in Sitges (1999), to be published in *World Scientific*.